Exp.-Nr.: A1/1–03
Eingang: 21. 12. 2003
an PAC:

Mainz Microtron MAMI

Collaboration A1: "Virtual Photons"

Spokesperson: H. Merkel

Proposal for an Experiment

Separation of transverse and longitudinal structure functions in $\mathbf{p(e, e'}\boldsymbol{K^+}\mathbf{)}\boldsymbol{\Lambda}$ at $\boldsymbol{W} = \mathbf{1.66\,GeV}$, $\boldsymbol{Q^2} = \mathbf{0.2\,(GeV/c)^2}$ in parallel kinematics

Collaborators:

P. Achenbach*, C. Ayerbe, D. Baumann, J. Bernauer, M. Ding, M. O. Distler, J. Friedrich, J. García Llongo, I. Goussev, D. v. Harrach, W. Heil, P. Jennewein, K. W. Krygier, M. Lloyd, H. Merkel, K. Merle, U. Müller, R. Neuhausen, L. Nungesser, A. Piegsa, J. Pochodzalla, Th. Walcher
(Institut für Kernphysik, Universität Mainz)

M. Potokar, S. Širca
(Institute "Jožef Stefan", Univ. Ljubljana, Slovenia)

* Contact person

Abstract:

We request 500 hours of beam-time for a commissioning experiment on kaon electroproduction. A measurement of the transverse and longitudinal structure functions in the $^1\mathrm{H}(\mathrm{e}, \mathrm{e}'K^+)\Lambda$ reaction will be carried out at four different values of the virtual photon polarisation. The data will be acquired at a kaon-hyperon centre-of-mass energy of 1.66 GeV and a squared four-momentum transfer of $Q^2 = 0.2\,(\mathrm{GeV/c})^2$. The structure functions will be separated through the detection of kaons along the direction of the virtual photon.

1 Introduction

Strangeness production is undergoing a renewed interest both experimentally and theoretically. Experimentally, there exist only few high quality data points on the reaction $e + p \rightarrow e' + K^+ + \Lambda$ at low energies, the available information on $K^+\Sigma^0$ electroproduction is even more sparse. On the theoretical side, due to the non-perturbative nature of QCD at low energies, kaon electroproduction in the MAMI-C regime is best described with effective Lagrangians, e.g. in chiral perturbation theory or isobaric models. In isobaric models the kaon production amplitudes are expressed in terms of hadronic degrees of freedom. The inherent assumption is that the amplitudes are dominated by the excitation and the decay of two-particle resonance states, called isobars. The interactions are then written in terms of an effective Lagrangian, in which the interaction strength is specified in a diagrammatic approach in terms of mesons and baryon exchanges and particle couplings. The coupling constants, i.e. the parameters of the model, are determined from performing phenomenological fits to the data (e.g. [WJC92, CWJ93, MB00]). Most of the kaon electroproduction models use single-channel approaches, in which a single hadron is exchanged, leading to tree-level diagrams as shown in Fig. 1. The model by Mart, Bennhold and colleagues [BHM99] was constructed focusing on dynamics in the s-channel. Since many resonances may contribute in this channel, and models disagree on the relative importance of the resonances entering the calculation, many free parameters have to be fixed. In the Bennhold model only those resonant states were included which decay with a significant branching ratio into $K\Lambda$ final states: $S_{11}(1650)$, $P_{11}(1710)$ and $P_{13}(1720)$. This model can explain recent SAPHIR photoproduction data [SAP98] only with the additional inclusion of a previously unseen $D_{13}(1960)$ resonance, however, other models can explain the same data without this resonance. These states are predicted to leave a large signature in polarisation observables. At energies more than 1 GeV above threshold, Regge phenomenology provides a method for describing the data with very few free parameters [GLV00]. It is based on two t-channel exchanges with K and K^* trajectories. While the Regge model is suitable for the CEBAF energy range, in particular, the MAMI-C energy range is complementary.

An elegant description of data on kaon electroproduction close to threshold is provided by chiral perturbation theory [SM97]. Forthcoming data from Mainz will serve as a testing ground. The theory, very successful in the SU(2) sector, is extended to the three-flavour case by formulating the effective Lagrangian in terms of the octet of Goldstone bosons, Φ, and the ground state baryon octet, Ψ_B:

$$\Phi = \begin{pmatrix} \pi^0 + \eta & \pi^+ & K^+ \\ \pi^- & -\pi^0 + \eta & K^0 \\ K^- & \bar{K}^0 & -\eta \end{pmatrix}, \quad \Psi_B = \begin{pmatrix} \Lambda + \Sigma^0 & \Sigma^+ & p \\ \Sigma^- & \Lambda - \Sigma^0 & n \\ \Xi^- & \Xi^0 & -\Lambda \end{pmatrix}$$

However, while the expansion parameter for SU(2) is small, $M_\pi/4\pi F_\pi = 0.12$, the larger strange quark mass leads to a parameter $M_K/4\pi F_\pi = 0.43$ and the expansion of reaction amplitudes in kaon momenta will require more effort. Only one calculation of the $K^+\Lambda$ total cross-section from threshold to 100 MeV above has been performed so far, but calculations including higher order effects are expected for the coming years. Testing the framework of chiral perturbation theory in the kaon sector will shed new light on the spontaneous and explicit chiral symmetry breaking in quantum chromodynamics.

We intend to perform, as a commissioning experiment on kaon electroproduction in

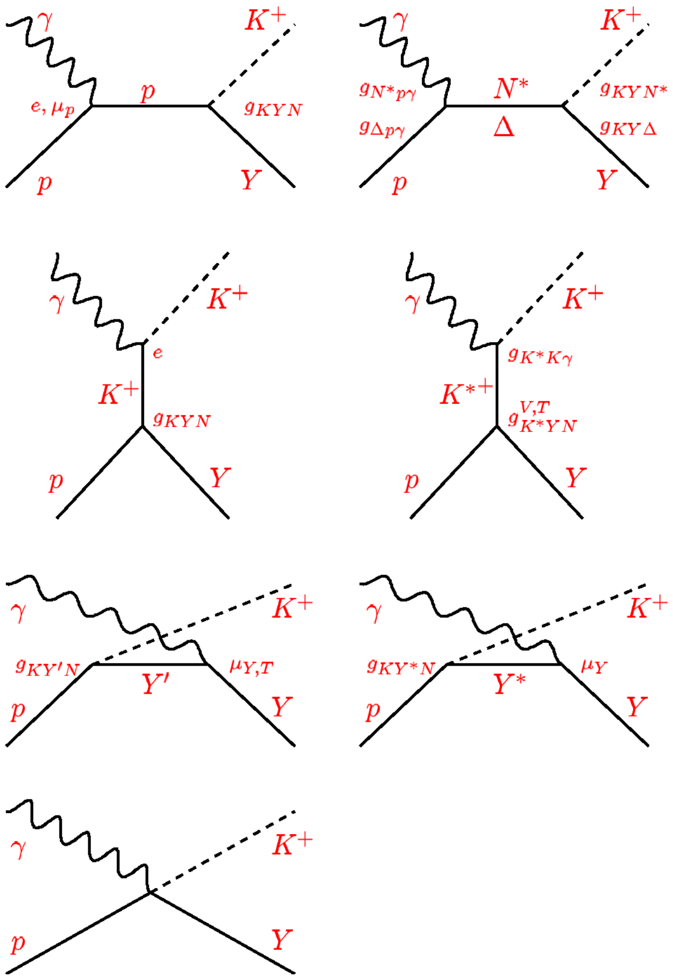

Figure 1: *The Born terms (left) and single-channel resonance terms (right) of isobaric models for kaon electroproduction. The first row shows s-channel diagrams, where nucleons and nucleon resonances contribute, the second row t-channel diagrams, where mesons contribute, and the third row u-channel diagrams with hyperon contributions.*

Mainz, the separation of transverse and longitudinal structure functions in parallel kinematics. Due to the lack of available data for the longitudinal component, σ_L, at low Q^2 and low W, a new precision measurement in this kinematical region should serve to constrain and refine isobaric models. This measurement shall become the starting point for a series of experiments on kaon electroproduction. Topics for future experiments are:

- the study of the spin degrees of freedom utilising the self-analysing nature of Λ hyperons in their weak decays $\Lambda \to p\pi^-$ [Hol95]; polarisation data is expected to provide sensitive tests of isobaric models that include different s-channel resonances, e.g. so-called "missing" resonances [MB00].

- the study of Λ hypernuclei; by measuring the kaon angular distribution, the bound Λ wave function inside the nucleus can be mapped out [Shi94, B$^+$99].

- the measurement of the Σ^0 channel; there is interest in the ratio of Σ^0/Λ transverse cross-sections, because it can be linked to the contribution of sea quarks to nucleon structure [Nac74].

- the study of the dependence of the longitudinal component on the Mandelstam variable $t = (q - K)^2$; the data can be used for determining the kaon electromagnetic form factor by extrapolating σ_L to the kaon pole at $t = m_K^2$ located in the unphysical region of positive t [MB98].

We will restrict the remainder of the proposal to the commissioning experiment.

2 Separation of the Structure Functions

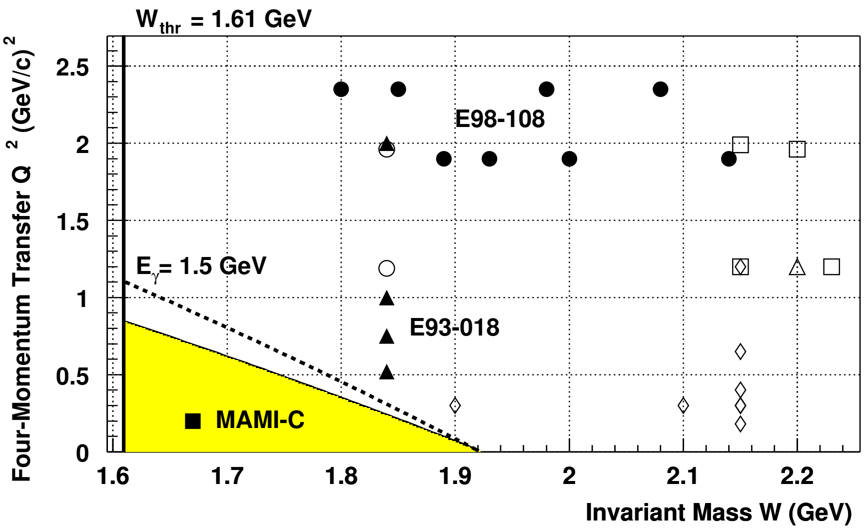

Figure 2: *Kinematics coverage by the world electroproduction data: open symbols are old data, solid triangles refer to Jlab experiment E93-018 and solid circles refer to Jlab experiment E98-108. The hatched triangle is the kinematical region accessible to MAMI-C, where the proposed kinematic setting is also shown.*

For unpolarised electrons and unpolarised target, the exclusive five-fold differential cross-section for the $\mathrm{p}(\mathrm{e}, \mathrm{e}'K^+)\Lambda$ process can be written in the general form (see e.g. [AFF79, DS78]):

$$\frac{\mathrm{d}\sigma}{\mathrm{d}\Omega \mathrm{d}E' \mathrm{d}\Omega_K^*} = \Gamma \frac{\mathrm{d}\sigma_v}{\mathrm{d}\Omega_K^*}, \tag{1}$$

where the virtual photoproduction cross-section is conventionally expressed as

$$\frac{\mathrm{d}\sigma_v}{\mathrm{d}\Omega_K^*} = \frac{\mathrm{d}\sigma_T}{\mathrm{d}\Omega_K^*} + \epsilon_L \frac{\mathrm{d}\sigma_L}{\mathrm{d}\Omega_K^*} + \sqrt{2\epsilon_L(1+\epsilon)}\, \frac{\mathrm{d}\sigma_{LT}}{\mathrm{d}\Omega_K^*} \cos\phi_K^* + \epsilon \frac{\mathrm{d}\sigma_{TT}}{\mathrm{d}\Omega_K^*} \cos 2\phi_K^* . \tag{2}$$

Here, the parameters for the transverse and longitudinal polarisation of the virtual photon are denoted by ϵ and $\epsilon_L = Q^2/\omega^{*2}\,\epsilon$, respectively, and the flux of the virtual photon field per scattered electron into $\mathrm{d}E'\mathrm{d}\Omega$ is given by the expression

$$\Gamma = \frac{\alpha}{2\pi^2} \frac{E'}{E} \frac{k_\gamma}{Q^2} \frac{1}{1-\epsilon} \quad \text{with} \quad k_\gamma = (W^2 - m_i^2)/2m_i\,. \tag{3}$$

There are a number of different conventions for how to define the longitudinal term. We have chosen to absorb the kinematic factor Q^2/ω^{*2} (with ω^* as the energy of the virtual photon in the hadronic centre-of-mass frame) into the structure functions and

make use of the transverse polarisation only. The kaon angles θ_K^* and ϕ_K^* are given in spherical coordinates in the hadronic centre-of-mass system. Other kinematic variables follow the standard definitions.
In parallel kinematics (3-momentum transfer parallel to kaon momentum) the interference terms σ_{LT} and σ_{TT} vanish due to their $\sin\theta_K^*$ and $\sin^2\theta_K^*$ dependence, respectively. The same is true for a measurement of the total cross-section, in which the ϕ_K^* angle is integrated over. Then, by varying ϵ_L, the longitudinal and transverse contributions can be disentangled by Rosenbluth separation. When keeping the hadronic invariant mass, W, and the squared four-momentum transfer, Q^2, constant, the variation must be accomplished by changing the beam energy.

3 Previous measurements

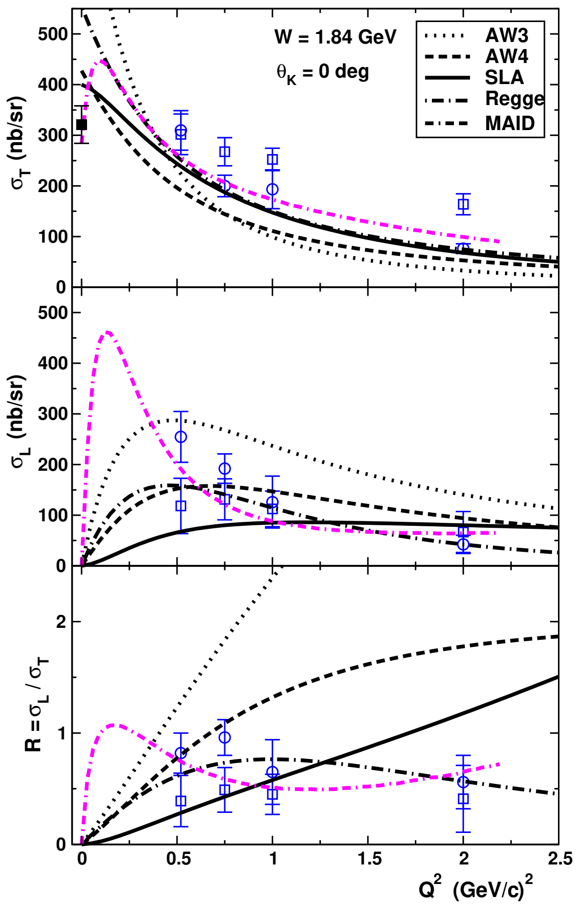

Figure 3: *The separated cross-sections σ_T and σ_L and their ratio R are shown as a function of Q^2 at $W = 1.84\,\mathrm{GeV}$ in parallel kinematics (from [BCF+03]). Predictions of some more elaborate models like Regge and MAID are plotted. The data points are from Jlab experiments E93-018 (circle) and E98-108 (square). No data is available for $Q^2 < 0.5(\mathrm{GeV/c})^2$.*

The main part of the kaon electro-production data-base comes from old experiments carried out in the 1970s at Cornell, DESY and CEA, and is of limited precision. A complete collection can be found, e.g. in [BBK+77]. A Rosenbluth separation was first applied to kaon electroproduction data from Harvard in 1977 [BBK+77]. Be-

cause of its poor statistics this experiment provided virtually no constraints for available theories and models. The same arguments holds for the 1979 data from DESY [BCC+79]. Additionally, the data were taken at values of W greater than 2 GeV. The first precise separation of cross-sections into longitudinal and transverse terms comes from the quite recent kaon electroproduction experiment E93-018 [N+98, M+03] carried out at Jefferson Laboratory in Hall C. E93-018 measured 12 data points (3 values of ϵ at 4 different values of Q^2) and achieved a precision of 45% in the separated cross-sections σ_L and 13% in σ_T at the smallest Q^2. Although, two different analyses of the data lead to different results (see p.11 of [M+03]) and no separation of cross-sections below $Q^2 = 0.5\,\mathrm{GeV/c}$ exists. Additional data points in the vicinity of the photon point would significantly improve the world data and resolve the remaining uncertainties. Experiment E98-108 in Hall A is expected to produce more data in a kinematical region of higher $Q^2 = 2.35\,(\mathrm{GeV/c})^2$ and $W \geq 1.80$ [Iod03]. Fig. 2 shows the $Q^2 - W$ kinematical region covered by the world published data so far (most data from E98-108 is preliminary). The measurements reached a number of conclusions about the production mechanisms. Probably most significant was the observation that both the transverse and longitudinal components of the cross-section contribute significantly to kaon electroproduction.
Fig. 3 (from [BCF+03]) shows latest experimental data on transverse and longitudinal cross-sections in ${}^1\mathrm{H}(\mathrm{e}, \mathrm{e}'K^+)\Lambda$ compared to some isobaric and one Regge model. Models AW3 and AW4 considered the nucleon resonances $P_{11}(1440)$, $S_{11}(1650)$ and the hyperon resonance $\Lambda^*(1670)$. The Saclay-Lyon model (SLA) includes some higher spin s-channel and four u-channel resonances. Predictions of the models differ significantly each other for both components of the cross-section at $Q^2 < 0.5\,(\mathrm{GeV/c})^2$. The MAID curve for the transverse part is constrained by the photoproduction point. The longitudinal component follows, as expected, the older data at small Q^2 shaping a pronounced bump structure at $Q^2 \approx 0.2\,(\mathrm{GeV/c})^2$. The bump structure in the cross-sections is created by the Dirac electromagnetic form factor F_1 of the missing $\mathrm{D}_{13}(1895)$ resonance which was assumed to be very steep at small Q^2. The ratio R is described satisfactorily only by the Regge and MAID models. More precise data for $Q^2 < 0.5\,(\mathrm{GeV/c})^2$ would be useful to supply additional constraints on the models and the contribution of missing resonances.

4 Apparatus

We require an unpolarised electron beam of 1.5 GeV with 10 μA current and a liquid hydrogen target. Spectrometer C will be used for detection of the scattered electrons. With the standard set-up of the three-spectrometer facility in Mainz, the detection of kaons under small scattering angles is not possible due to the short live-time of the kaons ($c\tau_K = 3.71\,\mathrm{m}$) and the long flight path through the spectrometers (close to 10 m for spectrometer C). Therefore, kaons are analysed at forward scattering angles with the KaoS spectrometer.

4.1 The KaoS spectrometer

KaoS is a very compact magnetic spectrometer suitable especially for the detection of kaons. It was built by the GSI in Darmstadt for heavy ion induced experiments. The relocation of the spectrometer from Darmstadt to Mainz was completed beginning of June 2003. It is currently being set-up in the spectrometer hall of the A1 collaboration. It is scheduled to be operational as soon as MAMI-C is delivering an electron beam of 1.5 GeV.

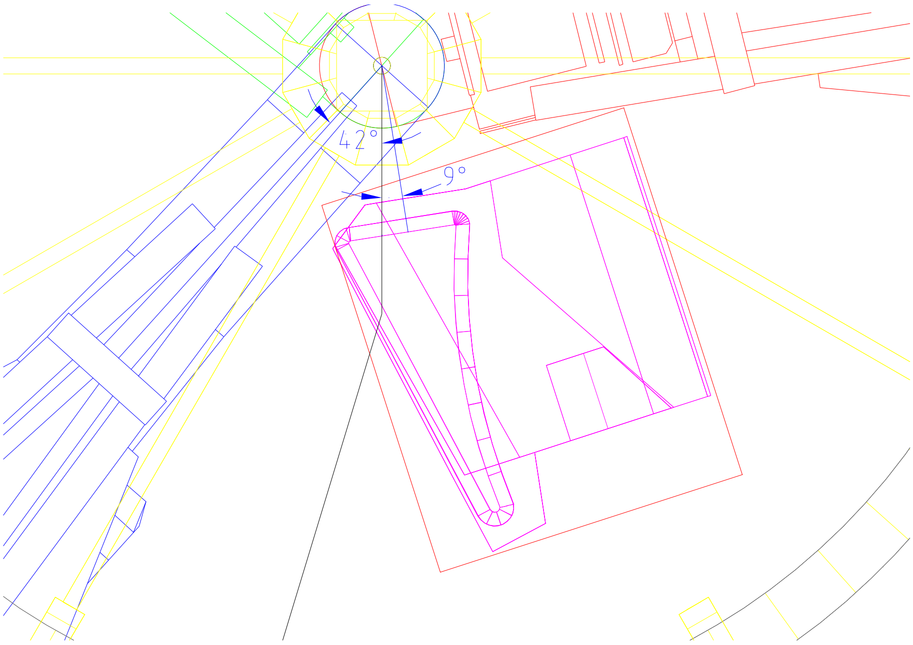

Figure 4: *Proposed experimental set-up for this measurement. The dipole is centred at 9° to the beam line, the target distance is 1.5 m.*

At GSI the spectrometer was used as a combination of a quadrupole and a dipole magnet. The dipole has a gap of 20 cm and is operated at variable magnetic fields up to $B = 1.95\,\mathrm{T}$. At Mainz, the demand of kaon detection under very small angles led to an experimental set-up, where the dipole is centred at 9° to the beam line and the quadrupole is unused. The large aperture and the open design of the dipole will allow the transport of the primary beam through the magnet, leading to a deflection of 12.6°. The installation of a new exit beam line to the existing beam dump is investigated. Fig. 4 shows the planned set-up.

4.2 Detectors of the KaoS spectrometer

For the detection of kaons a detector package situated near the focal plane of the optical system will be used: multi-wire proportional chambers for particle tracking and segmented scintillator arrays for time-of-flight (TOF) measurement and trigger information. For the time being, only one side of the two-sided spectrometer will be equipped with detectors. Positively charged particles are focused at a well defined focal plane where they are ordered with respect to their momentum. The two chambers of 120 cm length each will be used for a reconstruction of the particle's trajectory.

The development of a new focal plane detector system based on scintillating fibres is carried out in Mainz. A modern multi-anode photomultiplier read-out and a fast data acquisition system have been chosen for highest counting rate capabilities. First results on timing resolution, light yield and multiplicity of two prototype hodoscopes each having 32 channel (128 fibres) are available. Mass production of scintillating fibre segments is scheduled for 2004.

5 Monte Carlo Simulation

5.1 Method

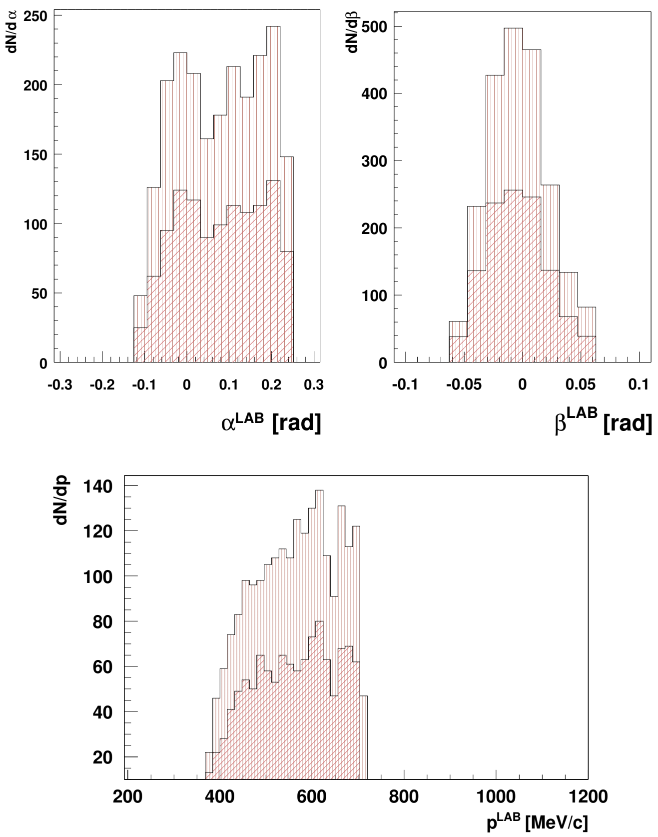

Figure 5: *Angular acceptance in the dispersive plane (α) and the non-dispersive plane (β) as well as momentum acceptance of the spectrometer for a field of 1 T. The dipole is centred at 9° to the beam line. The hatched curves require the detection of the kaon in the focal plane, and a coincidence with a detection of the electron in spectrometer C, respectively.*

The code used for this experiment is largely based on the Geant4 [GEA03] package. The simulation includes radiation, multiple scattering, and energy loss of the particles traversing the detectors. The acceptance function of the coincidence spectrometer set-up was extracted from the simulation. Fig. 5 shows the angular acceptance in the dispersive plane (α) and the non-dispersive plane (β). The hatched curves require detection of the kaon in the focal plane, and a coincidence with the detection of the electron in spectrometer C at -41.8°, respectively. The solid angle acceptance for kaons is calculated in this set-up to be 35 msr. The acceptance depends on the distance of the spectrometer from the target. We have chosen a distance of 1.5 m to allow a minimum angle between KaoS and spectrometer C of 40°. With an instrumented length of the focal plane of 1.5 m a momentum bite of $p_{max}/p_{min} = 1.75$ can be analysed with one field setting. Fig. 5 shows the momentum acceptance for a field of 1 T.

In order to extract cross-section information and estimates of counting rates, the MAID model [MBHT] has been implemented for the kaon electroproduction. Each event generated by a phase space generator is weighted by the five-fold cross-section

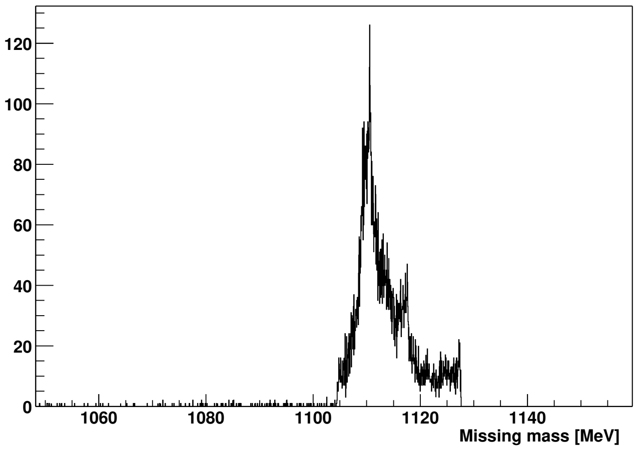

Figure 6: *Missing mass spectrum for this experiment as determined from a ray-tracing procedure with second-order coefficients and three measured coordinates in the focal plane detectors. The systematic errors in the used algorithm are responsible for the distinctive structures and is being replaced by a spline fit which is expected to reduce the errors. The* Λ *mass is* $m_\Lambda = 1116\,\mathrm{MeV}$.

$\mathrm{d}^5\sigma/\mathrm{d}\Omega_f \mathrm{d}E_f \mathrm{d}\Omega_K$. The MAID model is expected to provide an appropriate description of the separated cross-sections in the kinematical regions where data are available.
The necessary missing mass resolution for this kind of experiments can not be reached without ray-tracing of the particle's trajectory. Since the positions of both chambers and scintillator planes are not fixed, their set-up shall be optimised for highest resolution. Second-order transfer coefficients for a point-like target have been determined to study the missing mass resolution as function of target distance, detector positions and detector resolutions. A final conclusion cannot be drawn at the moment, but the resolution achievable with the existing detectors seems sufficient for this experiment. Fig. 6 shows the spectrum for one specific setting, where two position coordinates and one angular coordinate have been used for the ray-tracing. Systematic errors in the used algorithm for the determination of the transfer coefficients are responsible for the structures; the polynomial fit will be replaced by a spline soon, which is expected to reduce the errors.

6 Kinematics and counting rate estimates

Table 1: *Proposed kinematic settings for a measurement at invariant mass* $W = 1.66\,GeV$ *and squared four-momentum transfer* $Q^2 = 0.2\,(\mathrm{GeV/c})^2$.

Setting	Virtual Photon			Beam	Electron Arm		Hadron Arm	
	Q^2 $(\mathrm{GeV/c})^2$	W GeV	ϵ (trans.)	E_{MAMI} GeV	E' GeV	$\theta^{lab}(e')$ deg	$p^{lab}(K)$ GeV/c	$\theta^{lab}(K)$
1	0.2	1.66	0.32	1.40	0.28	-41.8	0.612	8.9
2	0.2	1.66	0.28	1.36	0.24	-46.1	0.612	8.3
3	0.2	1.66	0.23	1.32	0.20	-51.6	0.612	7.5
4	0.2	1.66	0.18	1.28	0.16	-59.2	0.612	6.6

For performing a longitudinal-transverse separation, it is important to have the lever arm in ϵ as large as possible. Obviously, the accessible ϵ range for fixed W is largest at small values of Q^2. We choose an invariant mass of $W = 1.66\,\mathrm{GeV}$ and a squared four-momentum transfer of $Q^2 = 0.2\,(\mathrm{GeV/c})^2$. The minimum electron scattering angle $\theta_e \geq 40°$ does not allow a measurement at values of ϵ above 0.32. The virtual photon flux decreases by orders of magnitude with increasing electron scattering angle. Therefore, we have limited the measurements to angles smaller 60 degrees. In table 1 the kinematic variables are listed in detail. To illustrate the kinematical coverage for a maximum beam energy of $E_{MAMI} = 1.5\,\mathrm{GeV}$ we present the accessible $Q^2 - \epsilon$ region in Fig. 7.

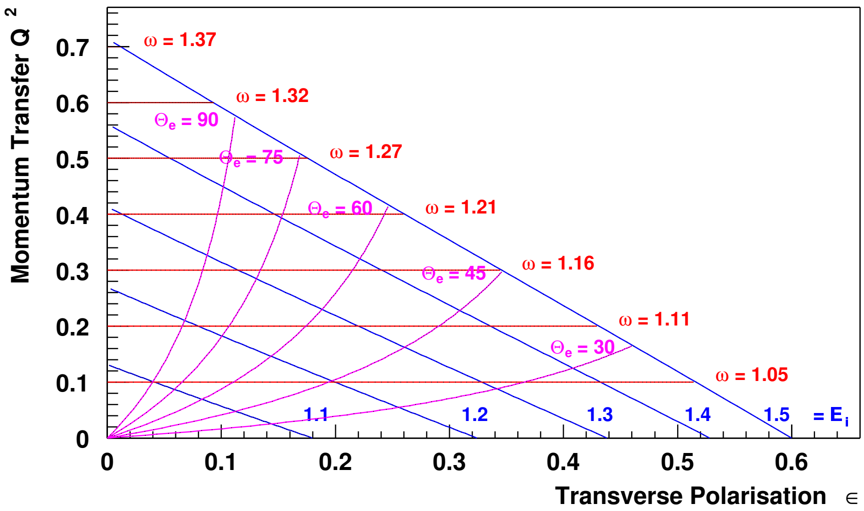

Figure 7: *The $Q^2 - \epsilon$ plane for a measurement at invariant mass $W = 1.66\,GeV$ and a maximum beam energy $E_{MAMI} = 1.5\,GeV$. Lines of constant scattering angle, θ_e, constant energy transfer, ω, and constant beam energy, E_i, are shown.*

Table 2: *Expected coincidence counting rates and proposed measuring times for $N \geq 10,000$ events per setting. Rates are calculated for the 28 msr collimator in spectrometer C, cross-sections by the MAID model [MBHT].*

Setting	Results from MAID + simu		e'K Coincidences		
	$\langle d\sigma/d\Omega_f\, dE'\, d\Omega_K \rangle$ $10^{-7}\,\mu b/sr^2/MeV$	$\alpha(K)$ %	Rate coinc/μC	Efficiency %	Measuring time hours
1	16.1	15.6	2.46	3	38
2	13.0	17.6	1.85	3	50
3	9.9	17.2	1.14	3	81
4	7.3	17.1	0.65	3	142
Σ					311

With the standard liquid hydrogen target a luminosity of $\mathcal{L} = N_{beam} N_{tgt} = 1.23 \cdot 10^{36}\,\mathrm{cm}^{-2}\mu\mathrm{C}^{-1}$ is attainable, where N_{beam} and N_{tgt} are the number of incident electrons and the number of target nucleons per cm^2, respectively. Assuming a moderate beam current of $10\,\mu\mathrm{A}$, for which the background radiation will have to be checked, a luminosity of $3.14 \cdot 10^7\,\mu\mathrm{b}^{-1}$ seems reasonable. For a satisfactory Rosenbluth separation, 10,000 true coincidences per measuring point will be necessary. The simulation including the MAID parametrisation [MBHT] for the cross-sections then gives the coincidence counting rates as shown in table 2.

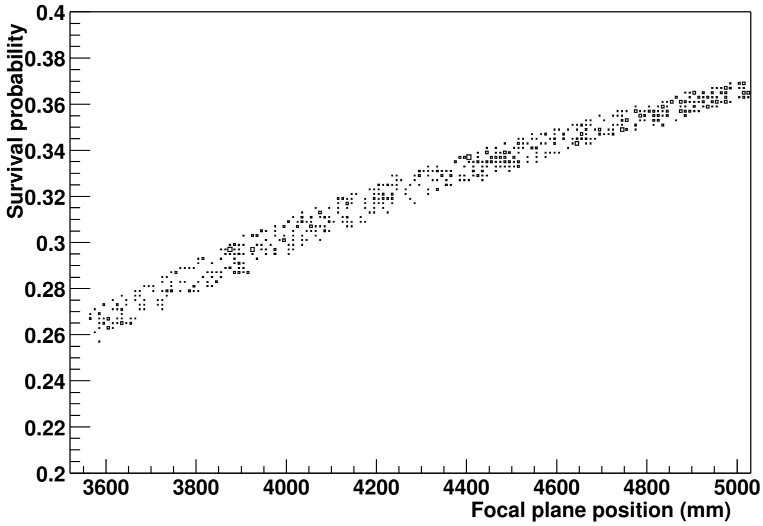

Figure 8: *Survival fraction of kaons detected in the focal plane.*

A large fraction of kaons created at the target will decay into secondary particles. Kaon survival fractions were determined from an exponential decay and the kaon flight times. Fig. 8 shows the survival fraction $P(l,p) = \exp(-m_K/\tau_K \times l/p)$ of kaons detected in the focal plane, where l is the flight length and p the momentum. The average number of $P \approx 30$ per cent is sufficiently large to allow for a cross-section correction with high accuracy ($1-3\%$ error). The simulation can also evaluate the possibility that a decay product might actually be detected.

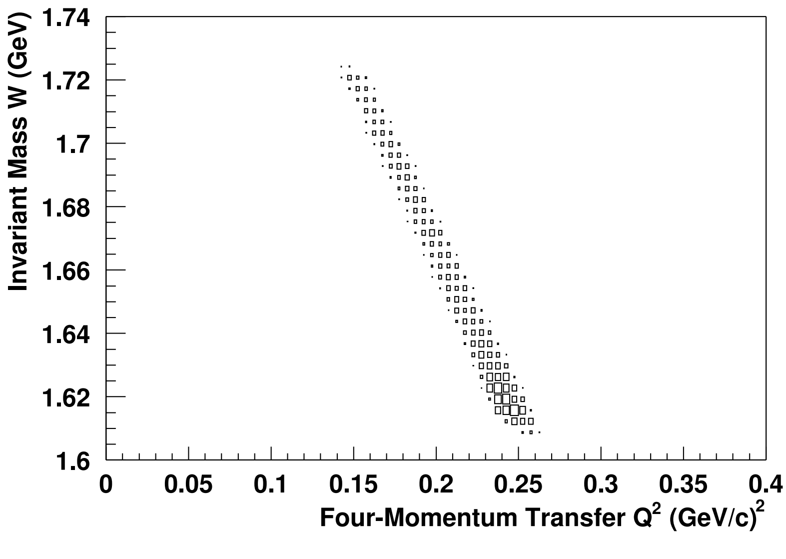

Figure 9: *The $W - Q^2$ acceptance of the proposed experimental set-up. Cuts on electron and kaon angles and momenta allow to derive the chosen kinematics.*

We assign the largest systematic effects on the counting rates to the kaon identification method. The estimate of cut efficiencies along with resulting systematic errors in the cross-sections is not easy to perform at this early stage of the experiment. If the spectrometer is set to accept all coincidences between a particle in its focal plane and an electron in spectrometer C we anticipate a contamination by particles not traversing properly the spectrometer, i.e. protons and electrons scattered into the focal-plane detectors, and random coincidences of the detectors due to background radiation. Fig 10 shows the flight time distribution for pions, kaons and protons assuming $\sigma = 1\,\mathrm{ns}$ timing resolution for the electron detector and $\sigma = 0.6\,\mathrm{ns}$ for the kaon detector, respectively. The used pion to kaon ratio was 1000:1. Three horizontal bands of electron coincidences with in-time particles are clearly identified. Random coincidences are not included. In order to generate a selective kaon trigger, a first-level particle identification has to be performed on-line. A cut on flight time shall be implemented as the main kaon identification method. For the specific purpose of rejecting the remaining pions we are investigating the use of an additional Čerenkov counter. The $W - Q^2$ acceptance of the proposed experimental set-up. Cuts on electron and kaon angles and momenta allow to derive the chosen kinematics. The trigger efficiency and the subsequent kaon identification efficiency is estimated to be about 15%. A concept for a better trigger on in-time particles is being investigated. The problem of random backgrounds will be addressed very soon by a measurement of the background radiation at the floor position of the focal plane detectors.

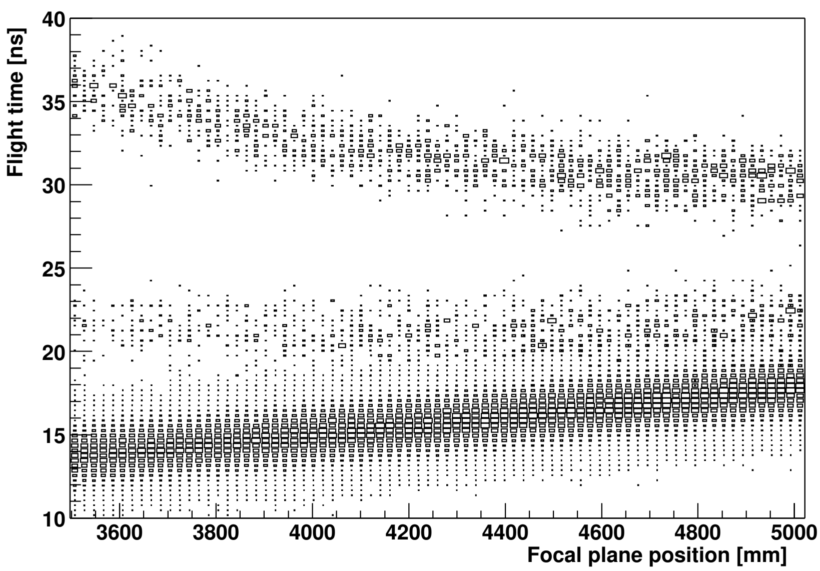

Figure 10: *Timing distribution of pions, kaons and protons (horizontal bands from bottom to top) in the focal plane of the spectrometer. A selective kaon trigger has to distinguish between the kaon and pion events.*

A total efficiency of $\epsilon_T = 3\%$ has been used in the calculation of the beam-time request, according to the following estimates: tracking and trigger efficiency ($\epsilon = 0.15$), reduced geometric acceptance ($\epsilon = 0.5$), *TOF* cut efficiency ($\epsilon = 0.7$), acquisition live-time ($\epsilon = 0.8$) and data acquisition dead-time ($\epsilon = 0.9$).

7 Beam-time request

We request 500 hours of beam-time as soon as MAMI-C is delivering an electron beam of 1.5 GeV. The main part of the set-up time is needed to install the spectrometer, the two chambers and the scintillators. The detectors, most of the electronics as well as the data acquisition can be checked without beam. A significant amount of beam-time (we have assumed 200 hours) is needed for the set-up of coincidence electronics, a test of the on-line kaon trigger and some calibration measurements.

References

[AFF79] E. Amaldi, S. Fubini, and G. Furlan. *Pion-Electroproduction*, volume 83 of *Springer Tracts in Modern Physics*. Springer, Berlin, 1979.

[B+99] C. Bennhold et al. Hypernuclear physics with photons. In *Workshop on Hypernuclear Physics with Electromagnetic Probes (HYJLAB99), 2–4 Dec 1999*, Hampton, Virginia, 1999. nucl-th/0011022.

[BBK+77] C. J. Bebek, C. N. Brown, R. V. Kline, F. M. Pipkin, S. W. Raither, L. K. Sisterson, A. Browman, K. M. Hanson, D. Larson, and A. Silverman. Scalar-transverse separation of electroproduced $K^+\Lambda$ and $K^+\Sigma^0$ final states. *Phys. Rev.*, D15:3082–3084, 1977.

[BCC+79] P. Brauel, T. Canzler, D. Cords, R. Felst, G. Grindhammer, M. Helm, W.-D. Kollman, H. Krehbiel, and M. Schädlich. Electroproduction of π^+n, π^-p and K$^+\Lambda$, K$^+\Sigma^0$ final states above the resonance region. *Zeit. Phys.*, C3:101, 1979.

[BCF+03] P. Bydžovský, F. Cusanno, S. Frullani, F. Garibaldi, M. Iodice, M. Sotona, and G. M. Urciuoli. Models for photo- and electro-production of K$^+$ in view of new data. 2003. nucl-th/0305039.

[BHM99] C. Bennhold, H. Haberzettl, and T. Mart. A new resonance in $K^+\Lambda$ electroproduction: The $D_{13}(1895)$ and its electromagnetic form factors. In *2nd ICTP International Conference on Perspectives in Hadronic Physics, 10–14 May 1999*, pages 328–337, Trieste, Italy, 1999. nucl-th/9909022.

[CWJ93] S. R. Cotanch, R. A. Williams, and C. R. Ji. Kaon electromagnetic production and radiative capture near hyperon thresholds. *Phys. Scripta*, 48:217–225, 1993.

[DS78] A. Donnachie and G. Shaw. *Electromagnetic Interactions of Hadrons*. Plenum, New York, 1978.

[GEA03] GEANT4 (S. Agostinelli et al.). Geant4: A simulation toolkit. *Nucl. Instrum. Meth.*, A506:250–303, 2003.

[GLV00] M. Guidal, J. M. Laget, and M. Vanderhaeghen. Electroproduction of strangeness above the resonance region. *Phys. Rev.*, C61:025204, 2000.

[Hol95] B. R. Holstein. Weak hypernuclear decay. 1995. nucl-th/9510048.

[Iod03] M. Iodice. Kaon electro-production on protons at JLab in Hall A. *Eur. Phys. J.*, A17:345–348, 2003.

[M+03] R. M. Mohring et al. Separation of the longitudinal and transverse cross sections in the $p(e,e'K^+)\Lambda$ and $p(e,e'K^+)\Sigma^0$ reactions. *Phys. Rev.*, C67:055205, 2003. nucl-ex/0211005.

[MB98] T. Mart and C. Bennhold. Kaon and hyperon form factors in kaon electroproduction on the nucleon. *Nucl. Phys.*, A639:237–246, 1998. nucl-th/9712012.

[MB00] T. Mart and C. Bennhold. Evidence for a missing nucleon resonance in kaon photoproduction. *Phys. Rev.*, C61:012201, 2000. nucl-th/9906096.

[MBHT] T. Mart, C. Bennhold, H. Haberzettl, and L. Tiator. An effective lagrangian model for kaon photo- and electroproduction on the nucleon. http://www.kph.uni-mainz.de/MAID/kaon/kaonmaid.html.

[N$^+$98] G. Niculescu et al. Longitudinal and transverse cross sections in the $^1\mathrm{H}(e, e'K^+)\Lambda$ reaction. *Phys. Rev. Lett.*, 81:1805–1808, 1998.

[Nac74] O. Nachtmann. On the ratio Σ^0/Λ in electroproduction off protons. *Nucl. Phys.*, B74:422, 1974.

[SAP98] SAPHIR (M. Q. Tran et al.). Measurement of $\gamma p \to K^+\Lambda$ and $\gamma p \to K^+\Sigma^0$ at photon energies up to 2 GeV. *Phys. Lett.*, B445:20–26, 1998.

[Shi94] S. Shinmura. Electroproductions of light lambda and sigma hypernuclei. *Prog. Theor. Phys.*, 92:571–582, 1994. nucl-th/9401017.

[SM97] S. Steininger and U.-G. Meissner. Threshold kaon photo- and electroproduction in SU(3) baryon chiral perturbation theory. *Phys. Lett.*, B391:446–450, 1997. nucl-th/9609051.

[WJC92] R. A. Williams, C. R. Ji, and S. R. Cotanch. Hyperon electroproduction in a crossing and duality constrained model. *Phys. Rev.*, C46:1617–1635, 1992.